

Effect of metal volume fraction on the mechanical properties of alumina/aluminum composites

N. A. TRAVITZKY

Advanced Ceramics Group, Technische Universität Hamburg–Harburg,

21073 Hamburg, Germany

E-mail: travitzky@tu-harburg.de

The influence of metal volume fraction on the mechanical properties of Al₂O₃/Al composites with constant diameter of metal ligaments was studied. Alumina/aluminum composites with interpenetrating networks and metal content between 12 and 34 vol.% were fabricated by gas-pressure infiltration technique. The fabricated composites exhibited good mechanical properties, e.g. the bending strength of 740 MPa for samples containing 12 vol.% of Al. The bending strength of the composites decreased with increasing volume fraction of metal phase. High strength of the fabricated composites was explained by strong interfacial bonding between alumina and aluminum. The fracture toughness of the composites increased, however, with increasing volume fraction of aluminum. The highest fracture toughness values of ~6 MPa √m were measured for the composites containing 25 vol.% of Al. Fractographic analysis of fractured surfaces showed deformed metal ligaments which demonstrated that crack bridging by plastic deformation of the metal phase is the main toughening mechanism in Al₂O₃/Al composites.

© 2001 Kluwer Academic Publishers

1. Introduction

Alumina, Al₂O₃, is a well studied and universally used ceramic material possessing such attractive properties as the excellent wear and oxidation resistance, good high temperature strength, etc. Their wider use, however, is limited by relatively low strength, fracture toughness and thermal shock resistance. It has been demonstrated, that incorporation of a ductile metal can considerably improve the mechanical properties of alumina. This type of composites feature microstructures that, with a few exceptions, are characterized by two interpenetrating phase networks: alumina and metal. Various processing techniques have been used to fabricate metal reinforced alumina. Infiltration (pressureless [1–7] and pressure-assisted (e.g., gas-pressure [8–11]) of porous Al₂O₃ performs by a liquid metal is one of the preferred techniques to fabricate this type of composites. For fabrication of alumina/metal composites by pressureless technique, the wettability of the alumina by the liquid metal was improved by additions of alloying elements [12, 13]. This is a case of Al₂O₃/Cu composites [4–6]. Pressureless infiltration of porous alumina preforms was obtained for copper-oxygen alloy containing 3.2 wt% of oxygen. Several recent reviews [14, 15] give general methods to enhance the wettability in metal-nonmetal systems. Problems usually arise with alumina/metal combinations where the wettability can not be improved by relatively simple treatment, e.g., Al₂O₃/Al. In this case, pressure has to be applied during infiltration [10].

The effective mechanism yielding the improved mechanical properties is crack bridging by the plastically deforming metal phase behind the crack tip [16–20]. Volume fraction of metal phase, size of ligaments, metal properties (ductility, work hardening, flow stress) and the interface properties may influence the toughening of ceramic/metal composites. Theoretical works [16, 21–23] suggest that fracture toughness will increase with metal volume fraction and bridge diameter. A simple model accounts for the influence of volume fraction and ligament diameter on the plateau toughness of Al₂O₃/Al composites [10]. In those works, however, changes in metal volume fraction are accompanied by changes in ligament diameter or different starting materials and processing routes were used to fabricate materials with the goal to study a separate influence of mentioned parameters on the mechanical properties of ceramic/metal composites.

The intention of present work was to study the influence of metal volume fraction on the mechanical properties of Al₂O₃/Al composites with constant diameter of metal ligaments.

2. Experimental technique

Alumina powder (Alcoa Chemicals, CT 3000 SG, 99.6 wt.% α-Al₂O₃, average grain size of ~0.5 μm) was used for the fabrication of porous ceramic preforms. Pure aluminum (99.9%, WAV, Germany) was used for infiltration. The as-received alumina powder was uniaxially pressed at a pressure of 50 MPa and then

cold isostatically pressed at 800 MPa to green compacts with dimensions of $45 \times 45 \times 7$ mm.

Green compacts were presintered in an electrically heated furnace in air at 1200, 1250, 1300, 1350 and 1400°C for 1 hour. The heating and cooling rates were $\sim 15^\circ\text{C}/\text{min}$. Each type of alumina filler preform was examined by mercury porosimetry. Densities were measured geometrically and by the Archimedes method using water as the immersion medium.

Alumina preforms to be infiltrated were mechanically fixed at the bottom of an alumina crucible and covered with aluminum. The system was heated in a HIP furnace in vacuum to 1000°C. Then, an Ar gas pressure of 15 MPa was applied for 10 min. forcing the molten Al to infiltrate into the alumina preform. On cooling, the pressure was kept up until aluminum had solidified.

The preforms and $\text{Al}_2\text{O}_3/\text{Al}$ composites were sectioned to bars with a diamond saw for mechanical testing and microstructure characterization.

The bending strength of the uninfiltrated and infiltrated bars ($3 \times 4 \times 35$ mm) was measured by four-point bending using spans of 30 and 10 mm. The tensile surface of the samples was polished up to a $0.25 \mu\text{m}$ finish.

Fracture toughness was measured by a chevron notch technique in four point bending [24]. In all the tests the crosshead speed was $50 \mu\text{m}/\text{min}$. A minimum of six samples were tested in each case in order to establish average values of bending strength and fracture toughness.

Vickers hardness was measured using a load of 100 N for duration of 15 s. An average hardness value was calculated using the results of 10 indentations. To enhance the optical contrast, a thin layer of gold was deposited by sputtering on the polished surfaces of the composites.

Young modulus and Poisson ratio of alumina porous preforms and $\text{Al}_2\text{O}_3/\text{Al}$ composites were measured by a dynamic method. For this test, plates with dimensions $35 \times 35 \times 5$ mm with highly parallel and polished opposite sides, were prepared. The longitudinal and transverse sound velocities were measured in the direction normal to the polished surfaces using ultrasonic equipment and transducers (10 mm diameter) with the center frequency of 10 MHz for both longitudinal and transverse waves. The thickness of the plate was measured with accuracy of 0.01 mm and the transient time could be measured with an accuracy of 5 ns. The pulse-echo method was used for calculating the velocity. Since the dimensions of the samples were much greater than the wavelength of an ultrasonic beam, expressions for plane strain conditions were used for calculations [25, 26].

The microstructure and phase composition of composites obtained were characterized by x-ray diffraction (XRD) and scanning electron microscopy (SEM). The samples for SEM analysis were relief-polished with a $0.05 \mu\text{m}$ alumina powder. The influence of presintering temperature on the grain and pore sizes of Al_2O_3 was estimated after infiltration. The grain and pore size were determined from average area measurements (an average of at least 1000 grains for each temperature).

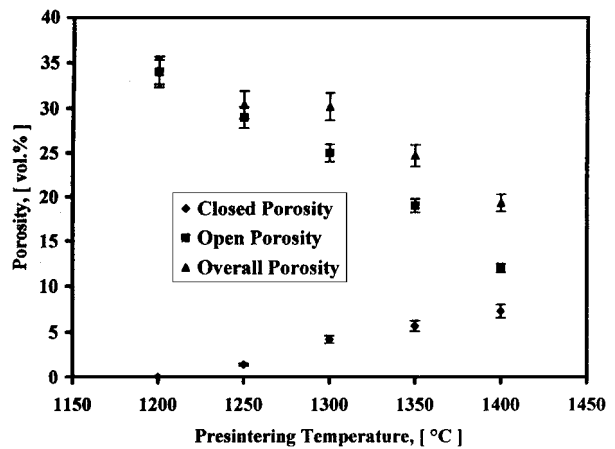


Figure 1 Influence of sintering temperature on porosity of alumina preforms.

3. Results and discussion

3.1. Microstructure

Presintering of alumina green compacts in an electrically heated furnace in air at 1200, 1250, 1300, 1350 and 1400°C for 1 hour resulted in the formation of preforms with open porosity of 34, 29, 25, 19 and 12 vol.%, respectively. The effect of sintering temperature on volume fraction of porosity in alumina preforms is shown in Fig. 1. An increase in volume fraction of closed porosity was observed with increase in sintering temperature. Fig. 2 displays the increase of Al_2O_3 grain size with sintering temperature. For instance, average grain sizes of 1 and $\sim 1.9 \mu\text{m}$ were measured for alumina presintered at 1200 and 1400°C, respectively. Only slight changes in open pore size between ~ 0.2 and $\sim 0.4 \mu\text{m}$, however, were observed with increase in sintering temperature from 1200 to 1400°C.

A nearly complete infiltration of all alumina preforms was obtained using the gas-pressure infiltration technique. X-ray diffraction analysis of Al_2O_3 preforms showed presence of mainly $\alpha\text{-Al}_2\text{O}_3$. Gas-pressure infiltration of alumina with aluminum resulted in composites containing mainly $\alpha\text{-Al}_2\text{O}_3$ and Al.

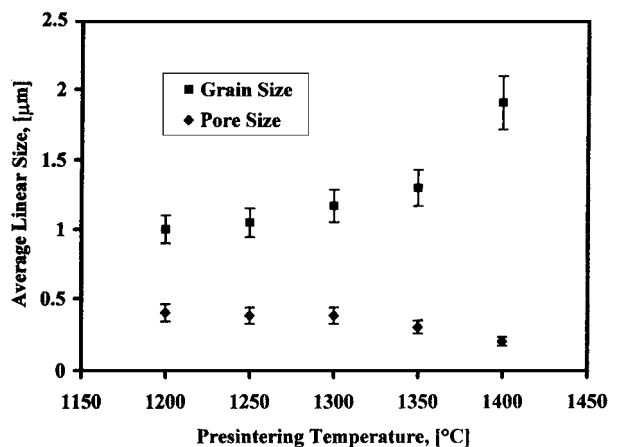


Figure 2 Influence of sintering temperature on grain and pore sizes of alumina preforms.

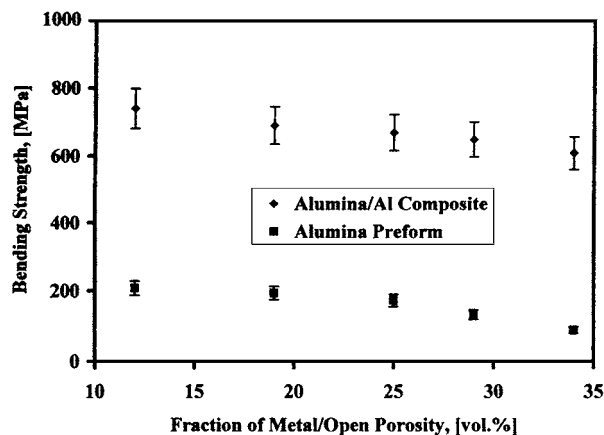


Figure 3 Bending strength of $\text{Al}_2\text{O}_3/\text{Al}$ composites and corresponding preforms.

3.2. Mechanical properties

Selected mechanical properties of the infiltrated alumina/aluminum composites are presented in Figs 3, 4, 6 and 7. The composites exhibit improved strength, fracture toughness, hardness and Young modulus. For comparison, the mechanical properties of uninfiltrated alumina preforms are also plotted.

Bending strength of Al_2O_3 preforms and $\text{Al}_2\text{O}_3/\text{Al}$ composites are presented in Fig. 3 as a function of initial porosity. In all cases, the strength of Al_2O_3 was considerably improved by infiltration with aluminum. The highest bending strength of 740 MPa is measured for the composite containing 12 vol.% of Al. It is believed that the results presented here due to the strong interfacial bonding between alumina and aluminum. Strong interfacial bonding leads to high geometrical constraint for the metal and high degree of triaxial tension in the metal ligament, thereby increasing the uniaxial yield strength by a factor of 5–7 [27]. High-resolution transmission microscopy (HRTEM) and analytical electron microscopy (AEM) were used to investigate the structure and chemistry $\alpha\text{-Al}_2\text{O}_3/\text{Al}$ interfaces in melt infiltrated polycrystalline alumina composites [28]. HRTEM combined with AEM showed the presence of Ca at embedded basal surfaces of $\alpha\text{-Al}_2\text{O}_3$. It was presumed that Ca segregates during sintering of alumina porous bodies. The presence of the surface phase with nominal composition correlating to the bulk phase $\text{CaO}\cdot 6\text{Al}_2\text{O}_3$ would be expected to alter the contact angle and wetting of Al on alumina, and can lead to the strong interfacial bonding. Since the decrease of metal volume fraction (preform open porosity) is accompanied by increase of bending strength of uninfiltrated alumina preforms by roughly constant ligament diameter (pore diameter), see Fig. 2, it is believed that both effects contribute to the strength increase of $\text{Al}_2\text{O}_3/\text{Al}$ composites.

Fig. 4 shows the dependence of fracture toughness on initial porosity for aluminum infiltrated and uninfiltrated alumina preforms. In all cases, the fracture toughness of Al_2O_3 was considerably improved by infiltration with aluminum. The highest fracture toughness values of $\sim 6 \text{ MPa}\sqrt{\text{m}}$ are measured for the composites containing 25 vol.% of Al. Fig. 5a shows the fracture surface of

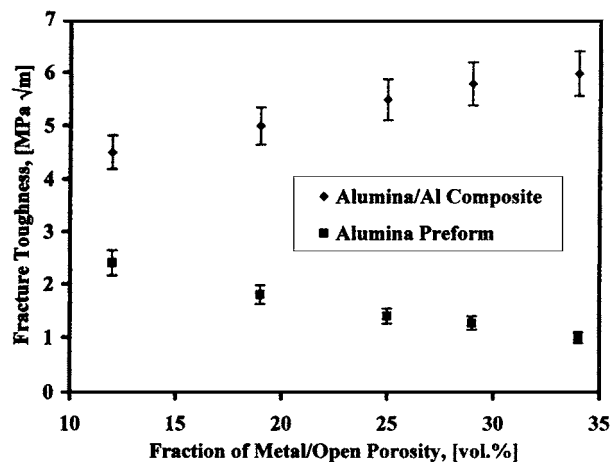
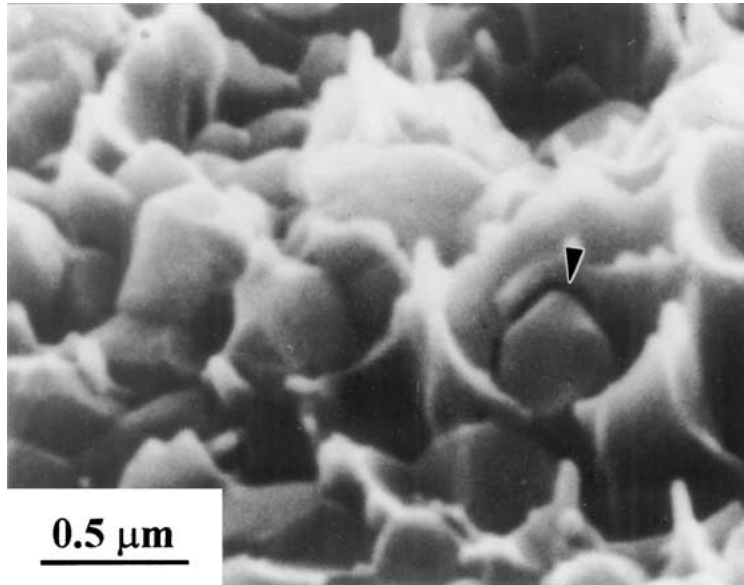


Figure 4 Fracture toughness of $\text{Al}_2\text{O}_3/\text{Al}$ composites and corresponding preforms.

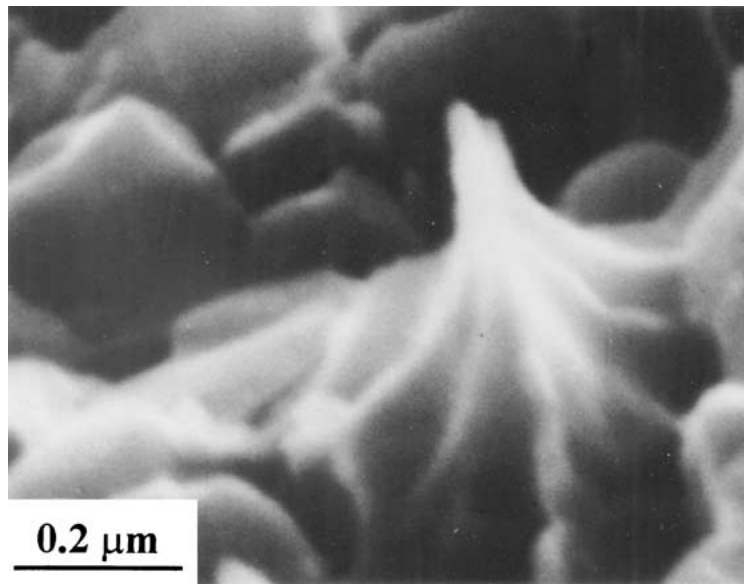
$\text{Al}_2\text{O}_3/\text{Al}$ composite (preform presintered at 1300°C). An aluminum network around alumina grains, is typical of all $\text{Al}_2\text{O}_3/\text{Al}$ composites. The existence of such a continuous aluminum network may increase the toughening effect of aluminum and allow crack propagation along this network. The aluminum phase has plastically deformed to sharp edges in a completely ductile manner (light phase in Fig. 5b). Thus, it can be supposed, that aluminum solidified in this case in single-crystalline form and gains an extra-high plasticity. Strong bonding between aluminum and alumina is typical for this type of composites (Fig. 5a). As a result of strong bonding, alumina grains seem to have fractured mainly in the transcrystalline manner. With increasing Al content above 25 vol%, some debonding, however, was also observed. The debonding could lead to a small amount of intercrystalline fracture, which was also found in the composites. Crack bridging by a ductile metal phase may control the fracture toughness of this type of composites. Crack deflection [29] and process zone shielding [30] are other possible mechanisms; however, their toughening potential is believed to be small [16, 31].

Fig. 6 shows the effect of metal volume fraction on Vickers hardness of $\text{Al}_2\text{O}_3/\text{Al}$ composites. The low hardness of composites with large metal contents is, apparently, due to the low fraction of the hard alumina phase forming a relatively weak network. As a result, mutual sliding of alumina grains takes place under the indenter and plastic flow of the metal phase is allowed. With decreasing metal content the skeleton of alumina becomes stronger hampering the plastic flow of the metal phase. The latter leads to the rise of quasi-hydrostatic stresses below the indenter, which significantly increases the resistance of material to indenter penetration. The highest hardness was, therefore, measured in the composites with the lowest content (12 vol.%) of the aluminum.

Young modulus of $\text{Al}_2\text{O}_3/\text{Al}$ composites and Al_2O_3 preforms as measured by the ultrasonic technique are presented in Fig. 7. The elastic modulus of ceramic materials is known to depend on its porosity as well as the pore structure. The volume fraction of porosity and the pore size of alumina undergoes a continuous change during presintering [Figs 1 and 2]. While some



(a)



(b)

Figure 5 Fracture surface of $\text{Al}_2\text{O}_3/\text{Al}$ composite. The corresponding preform presintered at 1300°C . Debonding indicated by arrow (Fig. 5a). Aluminum (light phase) has plastically deformed to sharp edges (Fig. 5b).

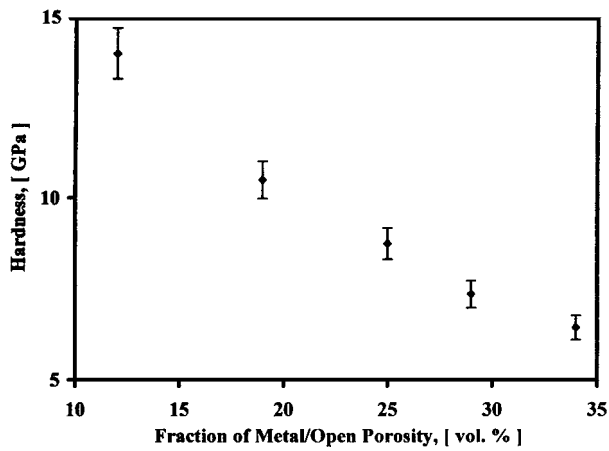


Figure 6 Influence of metal content on Vickers hardness of $\text{Al}_2\text{O}_3/\text{Al}$ composites.

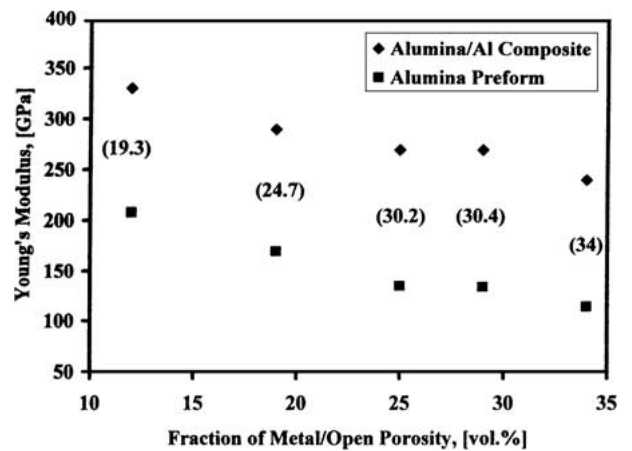


Figure 7 Young's modulus of $\text{Al}_2\text{O}_3/\text{Al}$ composites and corresponding preforms. Overall porosity (vol.%) is given in the brackets.

experimental investigators have observed elastic modulus to vary linearly over a finite range of porosity (21–49%) for a wide range of materials, there is no way to systematically predict the slope of this behavior from the porosity and zero-porosity modulus alone. Most of the empirical models, which have been proposed, contain one or more fitting parameters besides the porosity and zero-porosity modulus. More recently, experimental results indicating a significant departure from the linear modulus-porosity relation have been reported [32]. To describe non-linear elastic modulus-porosity behavior a semi-empirical relation was proposed if the assumption is made that Poisson ratio does not vary with porosity:

$$E = E_0(1 - aP)^n \quad (1)$$

where E and E_0 are the elastic moduli at porosity P and zero, respectively, and a and n are material constants [33]. The value of $a = 1$ indicates that Young modulus of the material becomes zero only at 100% porosity. Analysis of the overall porosity-elastic modulus data of alumina preforms yielded values of $a = 1$ and $n = 3$. The average value of $E_0 = 397$ GPa obtained from Equation 1.

The measured values of the elastic modulus of $\text{Al}_2\text{O}_3/\text{Al}$ composites are lower than that predicted from the rule of mixtures equations. This is, apparently, due to the residual closed porosity in the alumina network. Poisson's ratio remains roughly constant at 0.18 and 0.34 for uninfiltred and infiltred alumina, respectively.

4. Conclusions

$\text{Al}_2\text{O}_3/\text{Al}$ composites with different volume fraction and constant diameter of metal ligaments were fabricated by gas-pressure infiltration technique. The fabricated composites exhibited high mechanical properties. The bending strength of alumina/aluminum composites decreased with increasing volume fraction of metal phase. The highest bending strength of 740 MPa is measured for the composite containing 12 vol.% of Al. High strength of the fabricated composites can be explained by strong interfacial bonding between alumina and aluminum. The fracture toughness of the composites increased, however, with increasing volume fraction of aluminum. The highest fracture toughness values of ~ 6 MPa $\sqrt{\text{m}}$ are measured for the composites containing 25 vol.% of Al. Fractographic analysis of $\text{Al}_2\text{O}_3/\text{Al}$ composites revealed plastic deformation of Al, confirming that crack bridging by a ductile phase is the main toughening mechanism in these materials.

References

1. C. TOY and W. D. SCOTT, *J. Amer. Ceram. Soc.* **73** (1990) 97.
2. M. A. RITLAND and D. W. READEY, *Cer. Eng. Sci. Proc.* **14** (1993) 896.
3. X. M. XI and X. F. YANG, *J. Amer. Ceram. Soc.* **79** (1996) 102.
4. N. A. TRAVITZKY and A. SHLAYEN, *Mater. Sci. Eng.* **A244** (1998) 154.
5. E. J. GONZALEZ and K. P. TRUMBLE, *J. Amer. Ceram. Soc.* **79** (1996) 114.
6. N. A. TRAVITZKY, *Mater. Lett.* **36** (1998) 114.
7. N. A. TRAVITZKY, E. Y. GUTMANAS and N. CLAUSSEN, *ibid.* **73** (1997) 47.
8. N. TRAVITZKY and N. CLAUSSEN, *J. Eur. Ceram. Soc.* **9** (1992) 61.
9. S. WU, N. A. TRAVITZKY, A. G. GESING and NILS CLAUSSEN, *ibid.* **7** (1991) 277.
10. H. PRIELIPP, M. KNECHTEL, N. CLAUSSEN, S. K. STREIFFER, H. MUELLEJANS and M. RUEHLE, *J. Roedel A197* (1995) 19.
11. J. ROEDEL, H. PRIELIPP, N. CLAUSSEN, M. STERNITZKE, K. B. ALEXANDER, P. F. BECHER and J. H. SCHNEIBEL, *Scr. Met. et. Mat.* **33**(5) (1995) 843.
12. Y. V. NAIDICH, *Prog. Surf. Membr. Sci.* **1** (1981) 393.
13. G. A. HALDEN and W. D. KINGERY, *J. Phys. Chem.* **59** (1956) 557.
14. F. DELANNAY, L. FROYEN and A. DERUYTTERE, *J. Mater. Sci.* **22** (1987) 1.
15. S. Y. OH, J. A. CORNIE and K. C. RUSSEL, *Cer. Eng. Sci. Proc.* **8** (1987) 912.
16. L. S. SIGL, P. A. MATANGA, B. J. DALGLEISH, R. M. McMEEKING and A. G. EVANS, *Acta Metall.* **36** (1988) 945.
17. B. BUDIANSKY, J. C. AMAZIGO and A. G. EVANS, *J. Mech. Phys. Solids* **36** (1988) 167.
18. B. D. FLINN, M. RUEHLE and A. G. EVANS, *Acta Metall.* **37** (1989) 3001.
19. V. V. KRSTIC, P. S. NICHOLSON and R. G. HOAGLAND, *J. Amer. Ceram. Soc.* **64** (1981) 499.
20. C. A. ANDERSSON and M. K. AGHAJANIAN, *Ceram. Eng. Sci. Proc.* **9** (1988) 621.
21. K. S. RAVICHANDRAN, *Acta Metall. Mater* **42**(1) (1994) 143.
22. G. BAO and C.-Y. HUI, *Int. J. Solid. Struct.* **26**(5/6) (1990) 631.
23. A. G. EVANS and R. M. McMEEKING, *Acta Metall.* **34**(12) (1986) 2435.
24. D. G. MUNZ and J. L. SHANNON, *Int. Jour. Frac.* **16** (1980) R137.
25. P. J. SHULL and D. E. CHIMENTI, in "Review of Progress in Quantitative Nondestructive Evaluation," Vol. 118, edited by D. O. Thomson and D. E. Chimenti (Plenum, New York 1992).
26. D. BASU, S. MUKHERJEE and K. K. PHANI, *J. Mater. Sci.* **31** (1996) 1021.
27. M. F. ASHBY, F. J. BLUNT and M. BANNISTER, *Acta Metall.* **37**(7) (1989) 1847.
28. W. D. KAPLAN, H. MUELLJANS, M. RUEHLE, J. ROEDEL and N. CLAUSSEN, *J. Amer. Ceram. Soc.* **78**(11) (1995) 2841.
29. K. T. FABER and A. G. EVANS, *Acta Metall.* **31** (1983) 577.
30. A. G. EVANS and R. M. CANNON, *ibid.* **34** (1986) 761.
31. J. RODEL, *J. Eur. Ceram. Soc.* **10** (1992) 143.
32. L. P. MARTIN, D. DADON and M. ROSEN, *J. Amer. Ceram. Soc.* **79**(5) (1996) 1281.
33. K. K. PHANI and S. K. NIYOGI, *J. Mater. Sci.* **22**(1) (1987) 257.

Received 12 July 2000

and accepted 7 May 2001